





# VISTANet: Visual Spoken Textual Additive Net for Interpretable Multimodal Emotion Recognition

Puneet Kumar <sup>†</sup> , *Member, IEEE*, Sarthak Malik <sup>†</sup> , Balasubramanian Raman\* , *Senior Member, IEEE*, and Xiaobai Li , *Senior Member, IEEE*

**Abstract**—This paper proposes a multimodal emotion recognition system, Visual Spoken Textual Additive Net (VISTANet), to classify emotions reflected by input containing image, speech, and text into discrete classes. A new interpretability technique, K-Average Additive exPlanation (KAAP), has been developed that identifies important visual, spoken, and textual features leading to predicting a particular emotion class. The VISTANet fuses information from image, speech, and text modalities using a hybrid of early and late fusion. It automatically adjusts the weights of their intermediate outputs while computing the weighted average. The KAAP technique computes the contribution of each modality and corresponding features toward predicting a particular emotion class. To mitigate the insufficiency of multimodal emotion datasets labeled with discrete emotion classes, we have constructed a large-scale IIT-R MMemoRec dataset consisting of images, corresponding speech and text, and emotion labels ('angry,' 'happy,' 'hate,' and 'sad'). The VISTANet has resulted in 95.99% emotion recognition accuracy on the IIT-R MMemoRec dataset using visual, audio, and textual modalities, outperforming when using any one or two modalities. The IIT-R MMemoRec dataset can be accessed at [github.com/MIntelligence-Group/MMemoRec](https://github.com/MIntelligence-Group/MMemoRec)

**Index Terms**—Affective Computing, Emotion and Sentiment Analysis, Speech-Text-Image Signals, Information Fusion, Interpretable AI.

## 1 INTRODUCTION

THE multimedia data has grown in the last few years, leading multimodal emotion analysis to emerge as an important research trend [1]. It is used in various applications such as cognitive psychology, automated identification, intelligent devices, and human-machine interface [2]. Humans portray emotions through various modalities such as images, speech, and text [3]. Utilizing the multimodal information from them could increase the performance of emotion recognition [4]. Researchers have performed emotion recognition by analyzing visual, spoken, and textual information separately [5], [6], [7]. Multimodal emotion recognition using two modalities has been explored; however, it is yet to be fully explored using all three [4]. Moreover, most existing multimodal approaches do not focus on interpreting the internal workings of their emotion recognition systems [8].

Multimodal emotion recognition faces the unavailability of sufficient labeled data for training. Moreover, real-life multimodal data contains generic images with facial, human, and non-human objects, yet most existing datasets include only facial images [9]. In this context, perceived emotions, recognized by observers in multimodal content, differ from induced emotions which are reflected by the subjects themselves [10]. This paper focuses on perceived emotions because they more accurately reflect how individuals interact with and interpret real-world stimuli, a key aspect our proposed IIT-R MMemoRec dataset captures by including a variety of image types beyond facial expressions. A few multimodal datasets contain generic images; however, they consist

of positive, negative, and neutral sentiment labels instead of multi-class emotion labels [11], [12]. The IIT-R MMemoRec dataset contains generic images, corresponding speech utterances, text transcripts, and discrete labels: 'happy,' 'sad,' 'hate,' and 'anger.'

This paper proposes an interpretable multimodal emotion recognition system, VISTANet, which combines features from images, speech, and text using a hybrid of early and late fusion techniques. It utilizes a combination of complex pre-trained models along with simpler models. This configuration helps the simpler model learn and adapt by leveraging the robust knowledge of the pre-trained model, thus improving overall integration and responsiveness. A novel interpretability technique, KAAP, has also been developed to identify the important visual, spoken, and textual features that predict particular emotion classes. The VISTANet uses KAAP and automatically adjusts its intermediate outputs to compute the weighted average without human intervention.

An accuracy of 81.95% was observed for emotion recognition combining speech and text on the IIT-R MMemoRec dataset. The combinations of image and text, and speech and image, achieved accuracies of 86.40% and 84.66%, respectively. VISTANet outperformed these configurations by achieving a 95.99% accuracy when integrating all three modalities, underscoring the value of combining multi-modal information for emotion recognition. Further, the KAAP technique identifies the contributions of each modality and its features. The major contributions are as follows.

- A hybrid-fusion-based novel interpretable multimodal emotion recognition system, VISTANet, has been proposed to classify an input containing an image, corresponding speech, and text into discrete emotion classes.
- A novel interpretability technique, KAAP, has been developed to identify each modality's significance and the key image, speech, and text features contributing to recognizing emotions.
- A large-scale dataset, 'IIT-R MMemoRec dataset' containing images, speech utterances, text transcripts, and emotion labels has been constructed.

\* Corresponding Author.

<sup>†</sup> Contributed Equally.

P. Kumar is with the Center for Machine Vision and Signal Analysis, University of Oulu, Finland. Email: [puneet.kumar@oulu.fi](mailto:puneet.kumar@oulu.fi)

S. Malik and B. Raman are with Indian Institute of Technology Roorkee, India. E-mail: [sarthak\\_m@mt.iitr.ac.in](mailto:sarthak_m@mt.iitr.ac.in) and [bala@cs.iitr.ac.in](mailto:bala@cs.iitr.ac.in)

X. Li is with the Center for Machine Vision and Signal Analysis, University of Oulu, Finland, and the State Key Laboratory of Blockchain and Data Security, Zhejiang University, Hangzhou, China. E-mail: [xiaobai.li@oulu.fi](mailto:xiaobai.li@oulu.fi)

## 2 RELATED WORKS

### 2.1 Unimodal Emotion Recognition

In unimodal emotion recognition, individual modalities like speech, text, and images are utilized to detect emotions. Speech Emotion Recognition (SER) systems traditionally extract audio features such as cepstrum coefficients, voice tone, prosody, and pitch, key for identifying emotions [13]. These features distinctly categorize high-key emotions like happiness and anger from low-key emotions such as sadness and despair [14]. However, manual crafting required for acoustic features and the difficulties in parameter estimation pose challenges in developing robust SER systems [15]. Recent advances in deep learning techniques using spectrogram features and attention mechanisms have enhanced SER's effectiveness [16], [17]. Convolutional Neural Networks (CNNs) for spectrogram processing [18] and Recurrent Neural Network (RNN)-based techniques have shown promising results [7].

Text Emotion Recognition (TER) deals with analyzing emotions from online platforms such as YouTube, Facebook, and Twitter [19]. Attention mechanisms using graphs [20], transformer models [19], word embedding techniques from tweets [21], and graph network-based multimodal fusion [22] are some of the leading methods employed for TER. Sequence-based CNNs and the integration of semantic and emotional information enhance the modeling of textual emotions [23], [24]. Further, Image Emotion Recognition (IER) primarily utilizes facial expressions, leveraging techniques like face localization, micro-expression analysis, and landmark tracking. This modality benefits from both traditional low and mid-level image feature analysis and advanced deep learning approaches, including interpretable models and gamification in data collection [25], [5]. Despite its advancements, IER still faces challenges posed by deep learning techniques, highlighting the necessity for ongoing research in this area [5].

### 2.2 Multimodal Emotion Recognition

Emotion analysis using a single modality may not fully capture the emotional context [4]. Various modalities have distinct statistical properties, and recognizing complex emotions requires understanding the inter-relationships between them [2]. It has drawn researchers' attention to multimodal emotion analysis [26]. The existing works in this direction are discussed as follows.

Approaches that recognize emotions from speech utterances and corresponding text transcripts have been introduced, such as interpretability based on activation vectors [27] and separate acoustic and textual analyses to determine the emotional context [28]. Dual RNNs have been employed to extract audio and text information for emotion recognition [29], and transformers-based models have been fine-tuned to enhance performance [30]. Studies have also explored the simultaneous recognition of emotions in more than two modalities, employing information fusion techniques and developing end-to-end systems [31], [32]. In terms of recognizing emotional content in visual and textual modalities, researchers have developed semantic reasoning networks [33] and multi-task architecture-based approaches to handle missing modalities [34]. These efforts explore the interplay of visual and textual content using co-memory-based networks for sentiment recognition [35]. Further advancements include utilizing pre-trained transformers for multimodal integration [36], [37].

Multimodal emotion recognition approaches emphasize the integration of feature extraction and fusion techniques across visual, auditory, and textual modalities. Central to these advancements

are Transformer-based models, known for their ability to capture complex intermodal interactions. Ma et al. [19] introduced a Transformer model with self-distillation to enhance emotion recognition accuracy in conversational contexts, demonstrating the potential of Transformers to significantly boost performance by leveraging multimodal data. Zhang et al. [38] provided a systematic review of deep learning approaches for MER, highlighting the transformative impact of integrating modalities through advanced architectures like Transformers. In another work utilizing Transformers, Fan et al. [39] developed networks for depression detection by integrating diverse signals, showcasing the adaptability of this technology in affective computing.

Further advancements in the field have led to the development of methods for emotion classification that integrate fused speech and visual features [40], [41], alongside research focusing on modality-specific frameworks [42] and the incorporation of knowledge-embedded models for deeper analysis [43], [44], [45]. These classifications are also being employed in music recommendation systems using techniques like self-supervised learning of sound representations [46] and feature correlation analysis for emotion recognition [47].

### 2.3 Explainable and Interpretable Emotion Analysis

Explainability refers to the ability to describe an algorithm's mechanism leading to a specific output. At the same time, interpretability focuses on understanding the model's output context and analyzing its functional design [48]. Deep learning techniques, often acting as black boxes, have given rise to challenges in explaining and interpreting their workings, leading to the emergence of a new research area called explainable AI [49]. Riberio et al. [50] developed a method to identify which part of the input contributes to a particular output, and other research has traced the contributions of individual neurons to understand the output [51].

Existing interpretability techniques encompass three main categories: attribution-based, perturbation-based, and backpropagation-based methods. The latter two are further classifications of attribution-based methods. In attribution-based techniques, such as Shapley Values [52], attribution values are computed to signify the relevance of inputs to outputs. These methods are commonly employed for local interpretability, focusing on explaining the impact of individual instances rather than the entire model. Lundberg et al. [49] introduced the SHAP framework, utilizing Shapley values to determine each feature's contribution [8]. However, computing Shapley values can be computationally intensive, requiring training  $2^n$  models for a model with  $n$  features [49]. To mitigate this, approximations like KernelSHAP [49] and Shapley values sampling [53] have been proposed.

Perturbation techniques involve making small alterations to inputs and observing their impact on the model's behavior [54]. Local Interpretable Model-agnostic Explanations (LIME) [55] is a widely used perturbation technique that generates new data by perturbing the original instance and weights it based on proximity. Although applicable to any machine learning model, LIME's reliance on generating new data can lead to computational overhead. Backpropagation-based techniques compute attributions by iteratively backpropagating through the network. Saliency Maps [56] and Gradient-weighted Class Activation Map (Grad-CAM) [57] are prominent examples. Grad-CAM generates highlights of important input features by focusing on the last convolutional layer, thereby offering insights into model decisions [58].

As highlighted, techniques like LIME, SHAP, and Grad-CAM have challenges: LIME is computationally costly, Grad-CAM struggles with minor input changes, and SHAP, though robust, is mainly for visual modalities. These issues led to developing our KAAP interpretability technique for multimodal emotion recognition. Unlike traditional attention-based methods that highlight features without quantifying impact [6], [37], [44], KAAP offers a quantitative analysis of feature influence. It uses a perturbation-based method to evaluate contributions, providing precise insights into how modalities and features affect outcomes. This approach addresses limitations in attention-based models and enhances interpretability in multimodal emotion analysis.

### 3 PROPOSED WORK

#### 3.1 Data Compilation

The IIT-R MMEmoRec dataset contains generic (facial, human, non-human objects) images (as opposed to only facial images/videos in other multimodal datasets like IEMOCAP [9] and MOSEI [59]), speech utterances, text transcripts, emotion label ('angry,' 'happy,' 'hate,' and 'sad'), the probability of each emotion class. It has been constructed on top of the 'Balanced Twitter for Sentiment Analysis' (B-T4SA) dataset [12] which contains images, text, and sentiment ('positive,' 'negative,' neutral) labels. The IIT-R MMEmoRec dataset has discrete emotion labels for image, text, and speech modalities and it has been constructed as follows.

- The text from the BT4SA dataset is pre-processed by removing links, special characters, and tags, and then the cleaned text is converted to speech using the pre-trained state-of-the-art text-to-speech (TTS) model, DeepSpeech3 [60]. The rationale for using TTS is based on recent studies showing that TTS models produce high-quality speech, which can serve as a reliable approximation of natural speech [60], [61].
- The image and speech components are passed through a pre-trained VGG for IER and SER, respectively, while the text component is passed through a BERT for TER. The VGG was trained on the Flickr & Instagram (FI) [62] dataset and the IEMOCAP [9] dataset for IER and SER, respectively, while the BERT was trained on the ISEAR dataset [63] for TER. The prediction probabilities of each emotion class are obtained for each modality. For emotion recognition, we employed models distinct from those used in dataset construction, utilizing the VGG, trained on the ImageNet dataset, for visual and audio modalities, and the BERT (uncased L-12\_H-768\_A-12) for the textual modality.

TABLE 1: Class-wise data distribution.

Emotion	Samples
Angry	53,317
Happy	44,980
Hate	3,831
Sad	10,327

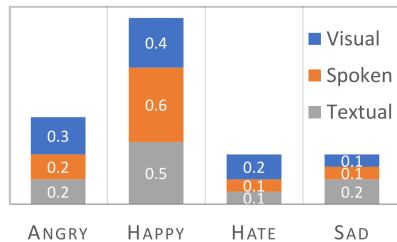


Fig. 1: Example of emotion label determination.

- The prediction probabilities are then averaged to obtain the ground-truth emotion of each data sample. The averaging is done to ensure that the chosen ground truth is the one that is supported by the majority of modalities. Fig. 1

shows an example of emotion label determination, whereas Table 1 describes the dataset's class-wise distribution. The probabilities for each emotion class given by each modality are shown. The 'happy' class has an average prediction probability of 0.500 compared to 0.233 for 'angry,' 0.133 for 'hate,' and 0.133 for 'sad.' The final emotion label for the sample is determined as 'happy.'


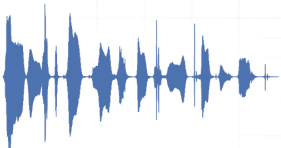

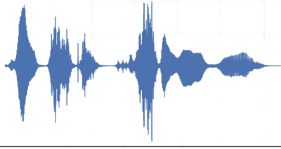

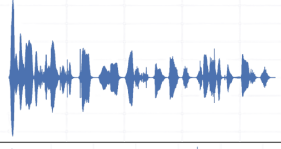
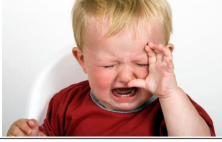
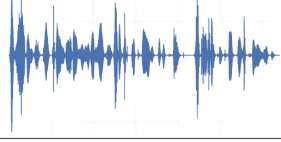
- The data is segregated according to classes, and the samples having an average prediction probability of less than the threshold confidence value of 0.55 times the maximum probability for the corresponding class are discarded. The threshold confidence is determined in Section 5.4.2.
- The four emotion classes, 'angry,' 'happy,' 'hate,' and 'sad,' are common in various datasets of different modalities considered in this work. Samples labeled as 'excitement' were merged with 'happy,' as excitement, categorized under 'surprise' in Plutchik's wheel of emotions [64], shares its positive valence. Similarly, samples labeled as 'disgust' were re-labeled as 'hate,' aligning with their shared high arousal characteristic, while 'sad' denotes low arousal. The final dataset contains 112455 samples with 53317 labeled as 'angry,' 44980 as 'happy,' and 10327 & 3831 as 'sad' and 'hate' respectively. Table 2 shows samples from the IIT-R MMEmoRec dataset.

##### 3.1.1 Determining Threshold Confidence Value

The B-T4SA dataset consists of 470586 samples labeled as 'positive,' 'negative,' and 'neutral.' When constructing the IIT-R MMEmoRec dataset with discrete emotion labels ('angry,' 'happy,' 'hate,' 'sad'), it was crucial to retain only those samples with a high degree of confidence in their emotion classification. After processing the image, speech, and text components through respective emotion recognition models, we assessed each sample's confidence level in its respective class. To establish an optimal threshold for confidence, three key factors were considered:

- *Modality-Wise Agreement:* The chosen threshold should ensure the final emotion class with the highest *final\_prob* to have a minimum probability of 0.51, affirming a decisive classification without inter-modality conflict. For instances, where one modality supports a secondary emotion class, the threshold ensures that the *final\_prob* of this class remains below that of the primary emotion class supported by the other two modalities. This analysis mandates a threshold greater than 0.51 for the corresponding sample to be retained in the IIT-R MMEmoRec dataset.
- *Dataset Size:* Observations from Fig. 2a, indicate that until a threshold of 0.37, a significant number of samples are retained, suggesting a potential compromise in label confidence. Between thresholds of 0.37 and 0.6, there is a steep decline in sample retention, indicating a more stringent filtering of data quality. Above a threshold of 0.6, very few samples are retained. Hence, a dataset between 0.37 and 0.6 should be selected to have a balance of dataset size and quality.
- *Class Distribution Consistency:* It is imperative to maintain a class distribution in the resultant dataset that mirrors that of the original B-T4SA dataset. Fig. 2b shows that maintaining the threshold up to 0.33 preserves this distribution optimally, with thresholds up to 0.55 still acceptable before the distribution significantly diverges.

TABLE 2: A few samples from IIT-R MMEmoRec dataset. Here, ‘Img\_Prob,’ ‘Sp\_Prob,’ ‘Txt\_Prob,’ and ‘Final\_Prob’ are image, speech, text, and final prediction probabilities, whereas angry, happy, hate, and sad emotion labels are denoted as 0, 1, 2 & 3 respectively.

Image	Speech/Spectrogram	Text	Img_Prob	Sp_Prob	Txt_Prob	Final_Prob	Label
		Are These the black lives thugs you are talking about?	0: 0.7812 1: 0.1767 2: 0.0293 3: 0.0128	0: 0.3740 1: 0.0244 2: 0.5308 3: 0.0708	0: 0.9204 1: 0.0796 2: 0.0001 3: 0.0001	<b>0: 0.6919</b> 1: 0.0936 2: 0.1867 3: 0.0279	0 (Angry)
		Great start to the senior year!!	0: 0.2584 1: 0.1297 2: 0.1657 3: 0.4461	0: 0.0245 1: 0.8485 2: 0.0276 3: 0.0995	0: 0.0038 1: 0.9962 2: 0.0001 3: 0.0001	0: 0.0956 <b>1: 0.6581</b> 2: 0.0644 3: 0.1819	1 (Happy)
		Unbelievable images of dead mermaid washed up on beach, see shocking photos.	0: 0.0030 1: 0.0055 2: 0.9350 3: 0.0564	0: 0.0833 1: 0.0113 2: 0.8814 3: 0.0241	0: 0.9090 1: 0.0890 2: 0.0001 3: 0.0019	0: 0.3318 1: 0.0353 <b>2: 0.6055</b> 3: 0.0274	2 (Hate)
		Oh SJWs, your tears say more than your nonsensical drivels ever could. #StaySalty #CryMeARiver	0: 0.1777 1: 0.0371 2: 0.1389 3: 0.6463	0: 0.0414 1: 0.0595 2: 0.0600 3: 0.8389	0: 0.9447 1: 0.0553 2: 0.0001 3: 0.0001	0: 0.3879 1: 0.0507 2: 0.0663 <b>3: 0.4951</b>	3 (Sad)

Given these considerations, the intersection of recommended threshold ranges suggests a threshold of 0.55 as the most balanced choice. This value effectively harmonizes the needs for high confidence in data labels, adequate sample retention, and preservation of the original class distribution.

### 3.1.2 Human Evaluation

The IIT-R MMEmoRec dataset has been evaluated by having 8 people evaluate the data samples. We had two human readers (one male and one female) who spoke out and recorded the text components of the data samples. The evaluators listened to the machine-synthesized speech against the human speech recorded by the human readers and scored the contextual similarity between them on a scale of 0 to 100. The human evaluators also evaluated whether the data samples’ speech, image, and text components agree with the annotated emotion sample. The samples have been picked randomly, and the average of the evaluators’ scores has been reported in Table 3 where  $S_{ss-hs}$  denotes the percentage of evaluators reporting the synthetic speech (ss) to be similar to human speech (hs).  $S_{ss}$  &  $S_{hs}$  denotes the percentage of speech components of synthetic and human speech portraying the annotated emotion. Likewise,  $S_i$  and  $S_t$  denote the agreement of annotated emotion class by image and text components.  $S_{ss-i-t}$  and  $S_{hs-i-t}$  show the samples showing agreement of the annotated emotion class by all three modalities on considering synthetic and human speech, respectively.

We had two readers read the text of the data samples and called their output human-synthesized speech. 60.72% evaluators found the synthetic speech to be contextually similar to the human synthesized speech. 74.49% synthetic speech samples and 78.91% human synthesized speech samples were found to portray the annotated emotion labels. As per further observations, 69.26% images and 78.81% text components of the data samples correspond to the annotated emotion labels. Moreover, the evaluators also reported that 72.99% of the samples considering machine-synthesized

speech along with the corresponding text & image were in line with the determined emotion label, whereas this is comparable to the value of 76.74% on considering human synthesized speech along with the corresponding text & image.

### 3.1.3 Anthropomorphic Score based Evaluation

The Anthropomorphic Score, proposed by Jaiswal et al. [65], quantifies the human-like quality of synthesized speech compared to natural speech. It represents the ratio of SER accuracy with synthesized speech to that with real speech. We used it to assess the reliability of IIT-R MMEmoRec dataset’s speech component synthesized via TTS. To validate our approach, we tested it on two multimodal emotion recognition datasets: IEMOCAP [9] and MELD [66]. We conducted SER twice: initially using their real speech, and then using speech synthesized from their text via DeepVoice3—the same TTS model employed in constructing the IIT-R MMEmoRec dataset. We then computed Anthropomorphic Scores for both the IEMOCAP and MELD datasets, which yielded an average score of 0.94. This score approaching 1 confirms the reliability of TTS-generated speech utterances as a robust approximation of real speech in our dataset construction.

## 3.2 VISTANet

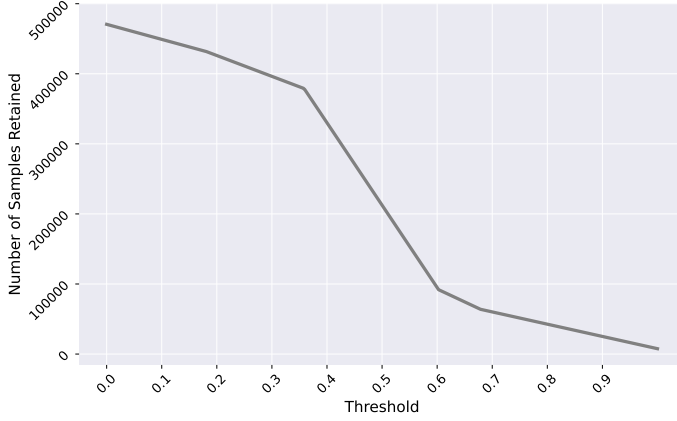
The proposed system, VISTANet’s architecture, is shown in Fig. 3, which has been decided based on the ablation studies discussed in Section 5.4.1. It fuses image, speech & text features using a hybrid of two-stage intermediate and late fusion, which considers all possible pairs of all three modalities and automatically weights them without human intervention. Intermediate fusion combines information from various modalities before classification, specifically after feature extraction, whereas late fusion combines information post-classification.

The three modalities are fed into two types of networks: pre-trained and simpler networks. The intuition behind this approach is to build a fully automated multimodal emotion classifier by

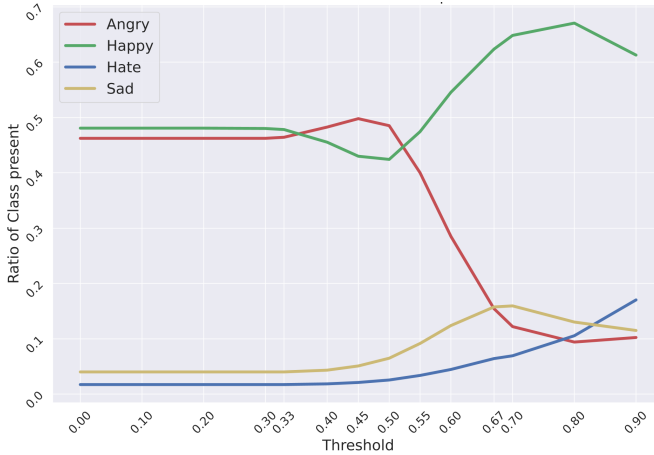


TABLE 3: Human evaluation of the IIT-R MMEmoRec dataset. Here  $S_{ss-hs}$  denotes the similarity between synthetic speech (ss) and human speech (hs) as reported by the evaluators. Likewise,  $S_i$ ,  $S_t$ ,  $S_{hs}$  and  $S_{ss}$  denote the reported agreement of annotated emotion class with image, text, human speech and synthetic speech inputs respectively.

Class	$S_{ss-hs}$	$S_{ss}$	$S_{hs}$	$S_i$	$S_t$	$S_{ss-i-t}$	$S_{hs-i-t}$
Angry	67.18%	82.81%	85.94%	70.31%	84.38%	75.00%	82.03%
Happy	52.78%	66.67%	69.44%	63.89%	72.22%	66.67%	69.44%
Hate	62.50%	71.43%	72.32%	67.86%	71.43%	73.21%	72.32%
Sad	60.42%	77.08%	78.13%	75.00%	87.50%	77.08%	83.33%
Overall	60.72%	74.49%	76.46%	69.26%	78.81%	72.99%	76.78%



(a) Number of data samples retained for different threshold values.



(b) Class-wise data distribution for different thresholds values.

Fig. 2: Determining threshold confidence for dataset construction.

including various modalities in all possible combinations and learning their weights while training without any human intervention. The proposed system contains  $P_i$  and  $S_i$  for image,  $P_s$  and  $S_s$  for speech, and  $P_t$  and  $S_t$  for text, denoting pre-trained and simpler networks, respectively. The input speech has been converted to a log-mel spectrogram before being fed into the network. A combination of complex pre-trained models has been employed with simpler, adaptable models to enhance the system's efficiency and adaptability. This setup mirrors a dynamic where a structured, rule-following member (complex pre-trained model) provides robust foundational knowledge, guiding a flexible, adaptable member (simpler model). This arrangement

allows the simpler models to adapt and apply these insights to new scenarios, thus maintaining the unique identity of each modality while optimizing overall system responsiveness. By leveraging the strengths of both model types, VISTANet ensures that learning is not only comprehensive but also sufficiently flexible, allowing for an effective integration of insights across different modalities.

### 3.2.1 Intermediate Fusion Phase

The images of dimension (128, 128, 3) are resized to (224, 224, 3) before being fed into  $P_i$  and  $S_i$  respectively.  $P_i$  comprises a VGG16 model [67] followed by a 512-dimensional dense layer, while  $S_i$  contains three convolution layers with 64, 128, and 256 filters of size (3, 3), followed by a dense layer of 512 dimensions. The spectrogram of size (128, 128, 1) from the speech input is initially processed through a convolution layer with 3 filters of size (3, 3) to enhance its feature extraction capability and to expand the channel depth to 3, making it compatible with the VGG16 model. This processed spectrogram is then further analyzed by  $P_s$  and  $S_s$ , which consists of the architecture as  $P_i$  and  $S_i$  respectively.

The text input is processed by  $T_i$ , which includes a BERT model [68], and  $T_s$ , which consists of an embedding layer followed by an LSTM layer with 64 units. Both  $T_i$  and  $T_s$  lead into 512-dimensional dense layers. In the intermediate fusion step, all pairs of pre-trained and simpler networks from different modalities are combined using a *WeightedAdd* layer that we have defined. This results in six distinct combinations, each processed through two dense layers with 1024 neurons, providing classification outcomes based on each pair. Equation 1 illustrates all possible pairings from the combination of pre-trained and simpler networks, ensuring that the networks in each pair do not belong to the same modality.

$$\begin{aligned}
 O_1 &= \text{WeightedAdd}(P_i, S_s) \\
 O_2 &= \text{WeightedAdd}(P_i, S_t) \\
 O_3 &= \text{WeightedAdd}(P_s, S_i) \\
 O_4 &= \text{WeightedAdd}(P_s, S_t) \\
 O_5 &= \text{WeightedAdd}(P_t, S_i) \\
 O_6 &= \text{WeightedAdd}(P_t, S_s)
 \end{aligned} \tag{1}$$

where  $O_1, O_2, O_3, O_4, O_5$ , and  $O_6$  represent the classification outputs for the pairs  $(P_i, S_s)$ ,  $(P_i, S_t)$ ,  $(P_s, S_i)$ ,  $(P_s, S_t)$ ,  $(P_t, S_i)$ , and  $(P_t, S_s)$ , respectively. The *WeightedAdd* layer ensures that during training, the weight of any weighted addition is learned using back-propagation without any human intervention. Each weight in the *WeightedAdd* layer is randomly initialized and passed from the softmax layer, giving us positive values used as final weights and learned during training.

### 3.2.2 Late Fusion Phase

In this phase, the information from various modalities' all possible pairs is combined in a hybrid manner. The intermediate classifica-

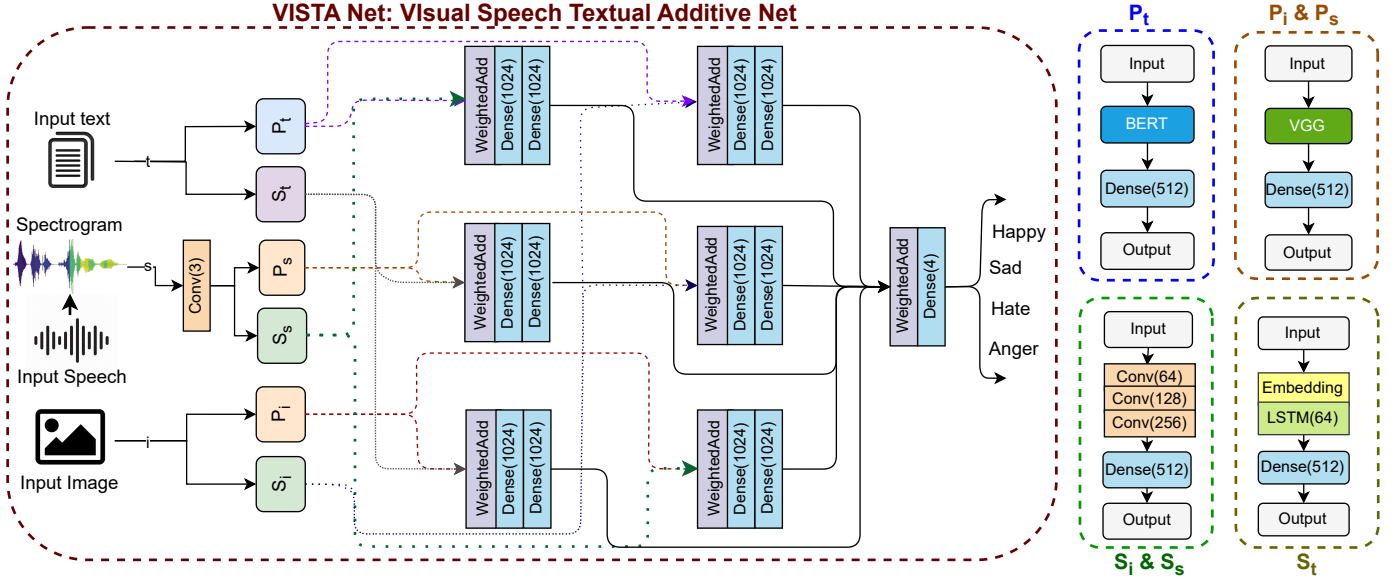


Fig. 3: Schematic architecture of the proposed multimodal emotion recognition system. Here,  $\mathbf{P}_m$  &  $\mathbf{S}_m$  denote the pre-trained & simpler networks for  $m^{th}$  modality whereas ‘i,’ ‘s,’ and ‘t’ denote visual, speech and text modalities, respectively.

tion outputs obtain(ed from above Eq. 1 are passed from another *WeightedAdd* layer, which combines these outputs dynamically, giving us the final output  $O$  as depicted in Eq. 2. The output  $O$  is passed from a dense layer with dimensions equal to the number of emotion classes, i.e., four.

$$O = \text{WeightedAdd}(O_1, O_2, O_3, O_4, O_5, O_6) \quad (2)$$

where  $O$  denotes the final output and  $O_1, O_2, O_3, O_4, O_5$  and  $O_6$  are the intermediate classification outputs. VISTANet dynamically learns the weight coefficients on a per-sample basis. Beyond averaging, it also learns to capture the interactions among different modalities, which is crucial for a more nuanced understanding.

### 3.3 KAAP

This Section proposes a novel multimodal interpretability technique, K-Average Additive exPlanation (KAAP), depicted in Fig. 4. It computes the importance of each modality and its features while predicting a particular emotion class. Most of the existing interpretability techniques do not apply to speech and multimodal emotion recognition. Moreover, the most frequently used and accepted interpretability technique for images and text is SHAP [49], which is an approximation of Shapley values [52]. It requires  $O(n^2)$  computational time complexity, whereas KAAP requires a time of  $O(k^2)$  where  $k \leq n$  is a given hyper-parameter. Moreover, KAAP applies to multimodal emotion analysis and a single modality or a combination of any two modalities.

#### 3.3.1 Calculating K-exPlanable Values

For a model with  $k$  features  $\{f_1, f_2, \dots, f_k\}$ , the K-exPlanable (KP) value of feature  $f_i$ , denoted  $kp_{f_i}$ , represents its importance. Fig. 5 depicts an example calculation. Consider four nodes: Node 1 with no feature, i.e., NULL; Node 2 with a single feature  $f_i$ ; Node 3 containing all remaining features from Node 1, i.e.,  $\{f_1, f_2, \dots, f_{(i-1)}, f_{(i+1)}, \dots, f_k\}$ ; and Node 4 with all the features  $\{f_1, f_2, \dots, f_{(i-1)}, f_i, f_{(i+1)}, \dots, f_k\}$ . The ‘Marginal

Contribution’ of an edge connecting Node  $i$  and Node  $j$  is defined as the difference between the prediction probabilities when using their respective features. For a given predicted label  $c$ , the marginal contribution of the feature  $f_i$  from Node 1 to Node 2 is calculated as per Eq. 3, where  $prob_{\{f_i\}}$  is the probability of label  $c$  calculated by using only feature  $f_i$  and setting all other features to zero.

$$MC_{f_i, \{f_i\}} = prob_{\{f_i\}} - prob_{\{\phi\}} \quad (3)$$

where  $\phi$  denotes a null feature. The overall importance of  $f_i$  is determined by calculating the weighted average of all ‘marginal contributions’ of  $f_i$  as shown in Eq. 4.

$$KP_{\{f_i\}}(k) = w_{12} \times MC_{f_i, \{f_i\}} + w_{34} \times MC_{f_i, \{f_1, f_2, \dots, f_k\}} \quad (4)$$

The weights  $w_{12}$  and  $w_{34}$  must satisfy two conditions: i) their sum equals one to normalize the weights; ii)  $w_{34}$  must be  $(k - 1)$  times  $w_{12}$ , reflecting the fact that  $MC_{f_i, \{f_i\}}$  represents the contribution of adding  $f_i$  to an empty set, while  $MC_{f_i, \{f_1, f_2, \dots, f_k\}}$  considers its contribution to a nearly complete set of features. These relations are formulated in Eq. 5 and calculated as shown in Eq. 6.

$$w_{12} + w_{34} = 1; \quad w_{12} = \frac{w_{34}}{k - 1} \quad (5)$$

$$w_{12} = \frac{1}{k}; \quad w_{34} = 1 - \frac{1}{k} \quad (6)$$

Eq. 7 show the KP values calculated using Eqs. 4 and 6.

$$KP_{\{f_i\}}(k) = \frac{1}{k} \times MC_{f_i, \{f_i\}} + \left(1 - \frac{1}{k}\right) \times MC_{f_i, \{f_1, f_2, \dots, f_k\}} \quad (7)$$

#### 3.3.2 Calculating KAAP Values

This Section computes the KAAP values and uses them to determine the importance of each modality and its features. The information of image, text, and speech modalities are in the same data format, i.e., continuous format. A single pixel can not define an object that can lead to a particular emotion for an image, but a group of pixels will. For speech, the spectrogram at a single

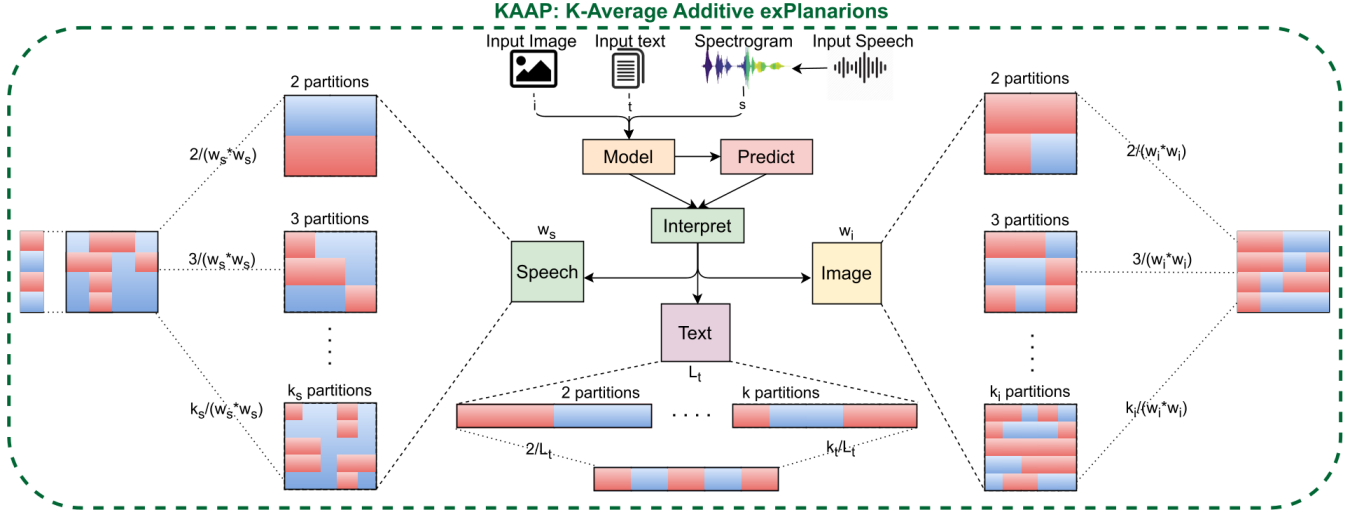


Fig. 4: Schematic representation of the proposed interpretability technique. The symbols  $k_i$ ,  $k_s$ , and  $k_t$  represent number of image, speech, and text partitions;  $w_i$ , and  $w_s$  are the widths for image & speech feature matrices, and  $L_t$  is the length of the text feature vector.

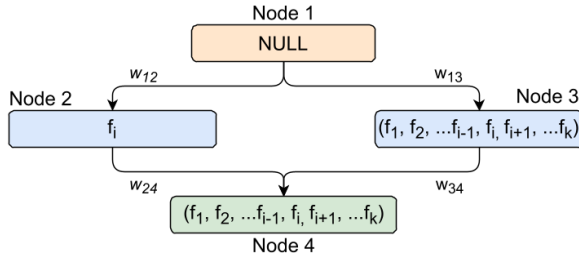


Fig. 5: Sample model for KP values computation.

instance of time & frequency alone can not define anything, but a time interval will. Likewise, for text, a single letter may not define an emotion, but a word can do so. KAAP values have been defined based on the motivation from the aforementioned fact. They are computed using the KP values for a group of features.

First, the input of size  $l$  is divided into  $k$  parts, where  $k$  is a hyperparameter decided through the ablation study in Section 5.4. These  $k$  parts correspond to the  $k$  features of the input. Then, for a feature group  $f_i$ ,  $KP_{f_i}(k)$  values are computed for the given value of  $k$  using Eq 6. It represents how a group of features  $f_i$  will perform compared to all remaining groups. However, these groups can vary in size, i.e.,  $k$  can have various values that lead to different groups and thus to different KP values from groups of different sizes, thus affecting the original features' importance. To deal with this issue, the weighted average of all the KP values is taken for  $k \in \{2, 3, \dots, k\}$  where weights are equal to the number of features in that group of features, given by the Eq. 8. It should be noted that  $k = 1$  is ignored here, as the whole input as one feature will not make any sense.

$$kaap_{\{f_i\}} = \sum_{j=2}^k \left[ \frac{j}{l} \times KP_{\{f_i\}}(j) \right] \triangleright \text{for linear feature} \quad (8)$$

For input image and speech spectrogram, both of width 128 and height 128, their KP values for a given  $k$  are calculated by dividing the input into  $k$  parts along both axes. As a matrix defines image and speech spectrogram, this gives us a  $k \times k$  feature group. The equation for calculating the KAAP values for the above two inputs is given by Eq. 9. It gives us a matrix showing the importance of each pixel for a given image and speech input. This matrix

directly represents the importance of the image. At the same time, for speech input, the values are averaged along the frequency axis to reduce the KAAP value matrix to the time axis, hence giving importance to speech at a given time.

$$kaap_{\{f_i\}} = \sum_{j=2}^k \left[ \frac{j^2}{w^2} \times KP_{\{f_i\}}(j) \right] \triangleright \text{for matrix feature} \quad (9)$$

For input text, the division is done such that each text word is considered a feature, as the emotion can only be defined by a word, not a single letter, as discussed above. Then, the text is divided into  $k$  parts, and as a linear array can represent text, the KAAP values are calculated using Eq. 8. Also, the value of  $k$  used for image, speech, and text modalities have been determined as 7, 7, and 5, respectively, in Section 5.4.2. Furthermore, the modalities' importance defined by symbols  $v$ ,  $\delta$ , and  $\tau$  for visual, spoken, and textual features, respectively, are computed assuming that image, speech, and text are three distinct features and calculating each modality's KAAP value for  $k = 3$ . While finding the importance of the features of a particular modality, all the other modalities are perturbed to zero.

## 4 IMPLEMENTATION

### 4.1 Experimental Setup

The network training for the proposed system has been carried out on Nvidia Tesla V100 GPU, whereas the testing & evaluation have been done on an Intel(R) Core(TM) i7-8700 Ubuntu machine with 64-bit OS and 3.70 GHz, 16GB RAM.

### 4.2 Training Strategy and Hyperparameter Setting

The model training has been performed using a batch-size of 64, with data partitioned into training, validation, and testing sets at ratios of 70%, 15%, and 15%, respectively, and evaluated using 5-fold cross-validation, *Adam* optimizer, *ReLU* activation function with a learning rate of  $1 \times 10^{-4}$  and *ReduceLROnPlateau* learning rate scheduler with a patience value of 2. The baselines and proposed models converged in terms of validation loss in 10 to 15 epochs. As a safe upper bound, the models have been trained for 50 epochs with *EarlyStopping* [69] with patience values of

5. The loss function is the average of categorical focal loss [70] and categorical cross-entropy loss. Accuracy, macro f1 [71], and *CohenKappa* [72] have been analyzed for the model evaluation.

### 4.3 Baselines and Proposed Models

The ‘Image + Speech + Text’ configuration described in Section 5.4.1 is considered as baseline 1, whereas further baseline models’ architectures have been formulated by incorporating further improvements in the information fusion mechanisms.

The baseline models are made on a common idea, as described below. Firstly, all three modalities are fed into  $P_i$ ,  $P_s$ ,  $S_i$ ,  $S_s$ ,  $T_i$  and  $T_s$  as described in Section 3.2, and are then passed from a dense layer of 512 neurons, resulting in a 512-dimensional outputs which are then combined using *WeightedAdd* to give three outputs. The following strategy is being followed for combining them: any pre-trained network must be combined with another simpler network. At least one combination must contain the network from different modalities because if all the modalities combine with themselves, then such a combination will not lead to any information exchange. Thus, six such configurations are possible, as described in Eq. 10.

$$\begin{aligned}
 (\#1) : & \{P_i + S_i, P_s + S_s, P_t + S_t\} \\
 (\#2) : & \{P_i + S_i, P_s + S_t, P_t + S_s\} \\
 (\#3) : & \{P_i + S_s, P_s + S_i, P_t + S_t\} \\
 (\#4) : & \{P_i + S_s, P_s + S_t, P_t + S_i\} \\
 (\#5) : & \{P_i + S_t, P_s + S_i, P_t + S_s\} \\
 (\#6) : & \{P_i + S_t, P_s + S_s, P_t + S_i\}
 \end{aligned} \tag{10}$$

The configuration (#1) is discarded as it does not hold the condition that at least one combination must combine with a different modality. The configurations (#2), (#3), (#6) are *partially-complete* combinations as one of the three outputs of these combinations combine the pre-trained and simpler network from the same modalities. On the other hand, the configurations (#4) and (#5) are *complete*.

Using the above strategy puts us in two disadvantages: i) only two out of five such baselines are complete while others are partially complete; ii) different datasets have different requirements. For example, a particular multimodal dataset may have better image and speech components, while other datasets may have a better quality of text components. To generalize for any dataset and scenario, an automated multimodal emotion recognition system, VISTANet, has been proposed, which combines all output of baselines 2-6, leaving any self-combination and taking the weighted average of remaining all. Hence, it automatically decides the weights of each combination according to the requirements of problem statements and the dataset. The results for baselines and the proposed system are summarized in the following Section.

## 5 RESULTS AND DISCUSSION

### 5.1 Quantitative Results

The VISTANet has achieved emotion recognition accuracy of **95.99%**. Its class-wise accuracies are shown in Fig. 6 while its results, along with the results of baselines, are shown in Table 4.

### 5.2 Qualitative Results

Sample emotion classification & interpretation results are shown in Fig. 7. The important speech and image features contributing to emotion classification are obtained, and corresponding words are highlighted. In the waveform, yellow and blue correspond to

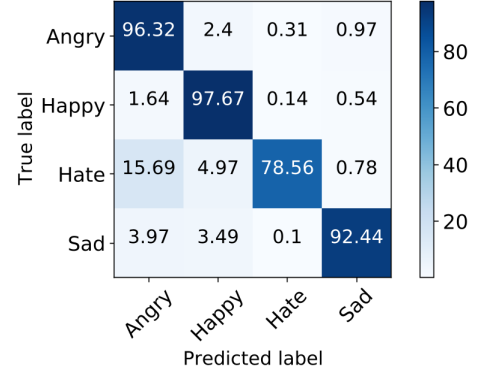


Fig. 6: Confusion matrix showing class-wise accuracies.

TABLE 4: Results comparison for emotion recognition on IIT-R MMEmoRec dataset. ‘Acc,’ ‘F1,’ ‘CK,’ ‘P,’ & ‘R’ denote accuracy, F1-score, CohenKappa score, precision & recall. Baseline 1 has (Image + Speech + Text) configuration from Section 5.4.1.

Model	Acc	F1	CK	P	R
Baseline 1	86.60	0.86	0.78	0.86	0.87
Baseline 2(#2)	94.89	0.95	0.91	0.95	0.95
Baseline 3(#3)	95.44	0.95	0.92	0.93	0.95
Baseline 4(#4)	95.39	0.95	0.92	0.95	0.95
Baseline 5(#5)	95.58	0.96	0.92	0.96	0.96
Baseline 6(#6)	95.37	0.95	0.92	0.95	0.95
VISTANet	<b>95.99</b>	<b>0.96</b>	<b>0.93</b>	<b>0.96</b>	<b>0.96</b>

the most and least important features, respectively. The speech and text were observed to be the most contributing modalities for the prediction of ‘angry’ and ‘hate’ classes, whereas image and text modalities contributed equally to the determination of ‘happy’ and ‘sad’ classes.

### 5.3 Results Comparison

#### 5.3.1 Emotion Recognition Results’ Comparison

Table 5 summarizes the emotion recognition results on the IIT-R MMEmoRec, IEMOCAP [9], and MELD [66] datasets for VISTANet and some state-of-the-art (SOTA) multimodal emotion recognition methods. It is important to note that VISTANet processes images for visual modality input, in contrast to some SOTA methods that utilize video inputs. To adapt SOTA methods for the newly proposed IIT-R MMEmoRec dataset, we replicated the same image to match the frame requirements of different methods. For instance, while MER-MULTI uses the average of all frames, we utilized the original image features directly. Conversely, the Multimedia Information Bottleneck (MIB) method aligns frames with the number of words in the text, requiring us to copy the image features as many times as there are words.

As observed from Table 5, VISTANet either outperforms or closely competes with the SOTA methods across all datasets. This underscores its capability to handle diverse emotional recognition scenarios effectively. Additionally, the successful application of SOTA emotion recognition methods on the IIT-R MMEmoRec dataset further validates its reliability and usefulness. Furthermore, the experiments conducted on the IIT-R MMEmoRec dataset are speaker-dependent, as all speech samples were generated using the TTS strategy described in Section 3.2. In contrast, the experiments on the IEMOCAP and MELD datasets are speaker-independent.



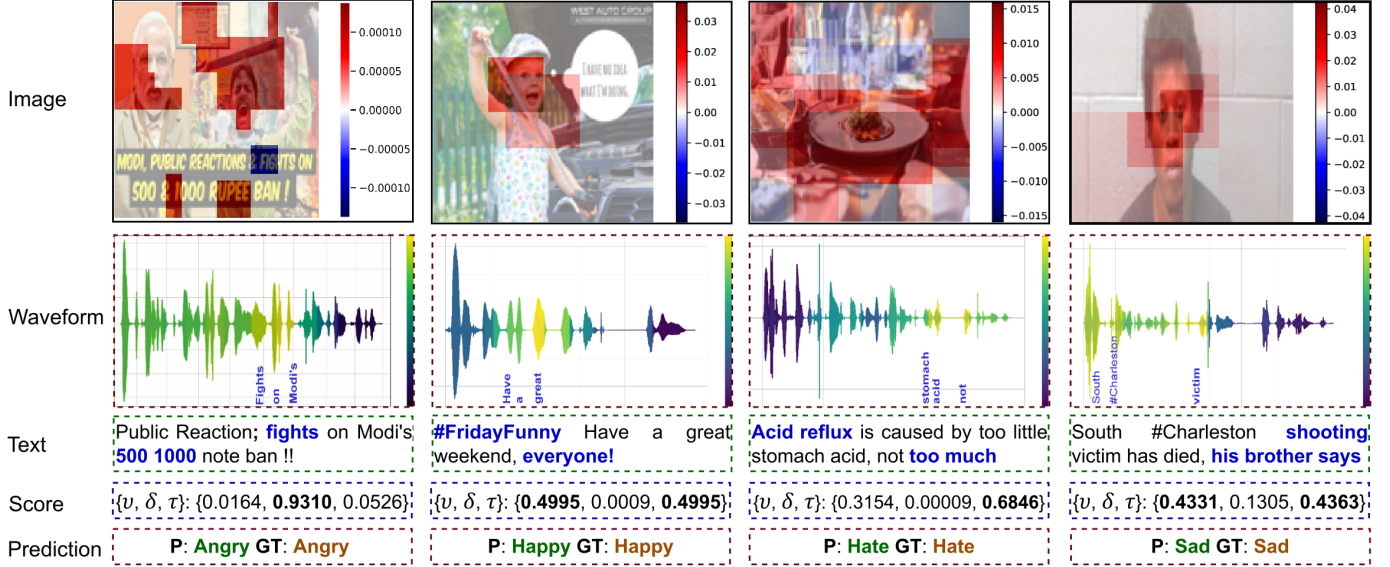


Fig. 7: Sample results; here, ‘P,’ ‘GT’ are the predicted and ground-truth labels whereas ‘Score’ denotes the importance of visual ( $v$ ), spoken ( $\delta$ ) & textual ( $\tau$ ) modalities.

TABLE 5: Comparison of results for emotion classification on the IIT-R MMEmoRec, IEMOCAP, and MELD datasets. The best and second-best results are marked in bold and underlined, respectively.

Approach	MMEmoRec	IEMOCAP	MELD
DialogueGCN [73]	–	65.25%	59.46%
MEmoBERT [43]	90.56%	65.74%	–
MER [44]	92.17%	66.13%	61.97%
DialogueCRN [74]	–	66.05%	60.73%
MM-DFN [75]	–	68.21%	62.49%
MIB [37]	93.12%	68.64%	–
UniMSE [41]	<u>94.23%</u>	<b>70.56%</b>	<u>65.09%</u>
VISTANet	<b>95.99%</b>	<u>69.42%</u>	<b>65.20%</b>

### 5.3.2 Sentiment Classification Results’ Comparison

The IIT-R MMEmoRec dataset has been constructed from the B-T4SA dataset in this paper; hence, there are no existing emotion recognition results for it. However, sentiment classification (into ‘neutral,’ ‘negative,’ and ‘positive’ classes) results on the B-T4SA dataset are available in the literature, which have been compared with VISTANet’s sentiment classification results in Table 6.

TABLE 6: Results comparison for sentiment classification on BT4SA dataset with existing approaches. Here, ‘V,’ ‘S,’ and ‘T’ denote visual, spoken and textual modalities.

Approach	Modality	Accuracy
Cross-Modal Learning [12]	V + T	51.30%
Multimodal Sentiment Analysis [11]	V + T	60.42%
Hybrid Fusion [76]	V + T	86.70%
Automated ML [77]	V + T	95.19%
VISTANet	V + S + T	<b>96.59%</b>

## 5.4 Ablation Studies

The ablation studies have been performed to determine the threshold confidence value for data construction, appropriate network configuration for VISTANet, and suitable  $k$  values for KAAP.

### 5.4.1 Ablation Study 1: Determining Baselines and Proposed System’s Architecture

To begin with, the emotion recognition has been performed for a single modality at a time, i.e., separate IER, SER, and TER using pre-trained VGG models [67] for Image & speech and BERT [68] for text. The performance has been evaluated in terms of Accuracy, CohenKappa metric (CK), F1 score, Precision, and Recall and summarized in Table 7. The CK metric measures whether the distribution of the predicted class is in line with the ground truth.

TABLE 7: Ablation Study 1. Here, ‘Acc,’ ‘F1,’ ‘CK,’ ‘P,’ and ‘R’ denote accuracy, F1-score, CohenKappa score, precision and recall.

Model	Acc	F1	CK	P	R
Image only	60.44	0.60	0.324	0.60	0.60
Speech only	78.69	0.75	0.624	0.74	0.79
Text only	81.51	0.81	0.69	0.81	0.82
Image + Text	86.40	0.86	0.77	0.86	0.86
Image + Speech	84.66	0.85	0.746	0.85	0.85
Text + Speech	81.95	0.81	0.70	0.82	0.81
Image + Speech + Text	<u>86.60</u>	<u>0.86</u>	<u>0.78</u>	<u>0.86</u>	<u>0.87</u>

Next, we moved on to the combination of two modalities. The chosen two modalities are fed into respective pre-trained models and then passed from a dense layer of 512 neurons. Then the information from these modalities is added using the *WeightedAdd* layer defined in 3.2.1. This output is next passed from three dense layers of size 1024, 1024, and 4 neurons, which then classifies the emotion.

Finally, the information from all three modalities is combined and fed into their respective pre-trained models and is then passed from a dense layer of size 512, which is then passed from a *WeightedAdd* layer; the output of this layer is passed from 3 dense layers as in the combination of two modalities. Combining all three modalities has performed better than the remaining models in all the evaluation metrics. As observed during the experiments above, combining the information from the complementary modalities has led to better emotion recognition

performance. Hence, the baselines and proposed model have been formulated, including all three modalities and various information fusion mechanisms in Section 4.3.

#### 5.4.2 Ablation Study 2: Determining $k$ Values for KAAP

An in-depth ablation study has been conducted here to decide the value of  $k$  used in Section 3.3.2. The dice coefficient [78] is used to determine the best  $k$  values. It measures the similarity of two data samples; the value of 1 denotes that the two compared data samples are completely similar, whereas a value of 0 denotes their complete dissimilarity. For each modality, KAAP values are calculated at  $k \in \{2, 3, \dots, 10\}$ . The dice coefficient is calculated for two adjacent  $k$  values. For example, at  $k = 3$ , the KAAP values at  $k = 2$  and  $k = 3$  are used to calculate the dice coefficient. The procedure mentioned above has been performed for all three modalities, and the results are visualized in Fig. 8.

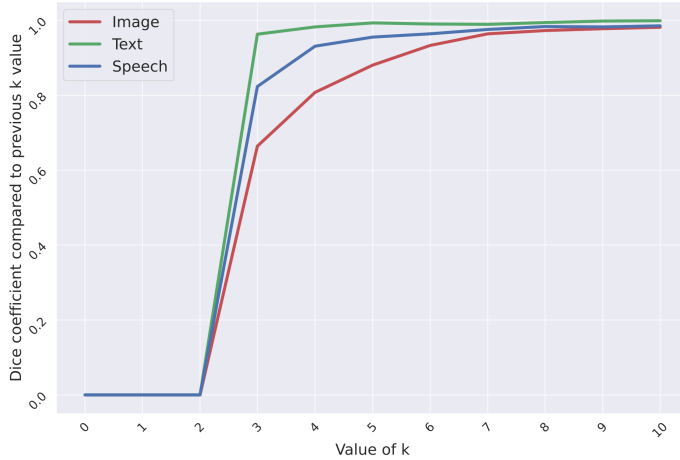


Fig. 8: Ablation Study 2: Determining appropriate  $k$  values.

The effect of increasing  $k$  values can be observed in the figure. For image & speech, the value converges to 1 at  $k = 7$ , while for text, the optimal value of  $k$  is 5.

#### 5.4.3 Ablation Study 3: Performance for Missing Modalities

In real-life scenarios, some data samples in the multimodal data may be missing information about one of the modalities. The VISTANet has been evaluated for such scenarios. We formulated four use cases with image, speech, text, or no modality missing and divided the test dataset into randomly selected equal parts accordingly. Then the information of the missing modality has been overridden to null, and VISTANet has been evaluated for emotion recognition.

TABLE 8: Results for missing modalities. ‘Acc,’ ‘P,’ ‘R,’ ‘F1,’ & ‘CK’ denote accuracy, precision, recall, F1 & CohenKappa scores.

Model	Acc	F1	CK	P	R
Missing Image	82.59	0.82	0.77	0.86	0.83
Missing Speech	57.62	0.45	0.75	0.75	0.58
Missing Text	62.82	0.68	0.70	0.87	0.63
Missing None	95.90	0.96	0.92	0.96	0.96

Table 8 summarizes the results. The emotion recognition performance for Missing no modality (i.e., having the information from all three modalities) aligns with the results observed in

Section 5.2. Further, missing image modality information has caused the least dip in the performance. Moreover, the information from speech and text modalities combined has resulted in an emotion classification accuracy of 82.59%, whereas including all the modalities resulted in 95.90% accuracy. The aforementioned observations align with the observations in Section 5.4.1 where IER performance was lesser than TER and SER performance.

## 5.5 Discussion

Various research tasks may require a particular modality’s information more than the others. For example, text and visual information may be secondary for multimodal speech recognition. Similarly, a multimodal emotion dataset might contain better quality information for one modality over others. Typically, human intervention would be needed to decide the importance of each modality. However, the VISTANet can determine this automatically, considering all possible combinations of modality information and weighing them accordingly.

As the proposed IIT-R MMEmoRec dataset contains information from complementary modalities, it enables deep learning models to learn the contextually related representation of the underlying emotions. The final label, considered the ground truth of the dataset, is derived by averaging the probabilities of each emotion obtained from unimodal models. Using the same unimodal models for dataset construction can introduce slight bias in performance, but no bias arises when developing and using a new multimodal emotion recognition model. Human evaluators also assessed the IIT-R MMEmoRec dataset for consistency in the determined emotion labels and the appropriateness of the synthesized speech component via text-to-speech.

The experimental results confirm the significance of using information from complementary modalities. As depicted in Fig. 7, different modalities play a crucial role in identifying the overall emotion conveyed by the input data. Some data samples might lack information from a specific modality. The proposed VISTANet system was tested in such scenarios, and the findings align with the insights from ablation studies.

The proposed interpretability technique, KAAP, computes the importance of each modality and the importance of their respective features towards the prediction of a particular emotion class. The existing interpretability techniques, such as SHAP and LIME, are not applicable to speech modalities, whereas KAAP is applicable to all image, text, and speech modalities. The proposed technique is expected to pave the way for growth in multimedia emotion analysis. We also hope the IIT-R MMEmoRec dataset will inspire further advancements in this context.

## 6 CONCLUSIONS AND FUTURE WORK

The proposed system, VISTANet, performs emotion recognition by considering the information from the image, speech & text modalities. It combines the information from these modalities in a hybrid manner of intermediate and late fusion and determines their weights automatically. It has resulted in better performance on including image, speech & text modalities than including only one or two of these modalities. The proposed interpretability technique, KAAP, identifies each modality’s contribution and important features toward predicting a particular emotion class. The future research plan includes transforming emotional content from one modality to another. We will also work on controllable emotion generation, where the output contains the desired emotional tone.

## ACKNOWLEDGEMENTS

This work was initiated at the Machine Intelligence Lab, Indian Institute of Technology Roorkee, India, and extended at the Center for Machine Vision & Signal Analysis, University of Oulu, Finland. This work was supported by the University of Oulu & Research Council of Finland Profi 5 HiDyn fund (grant 24630111132). The authors also acknowledge the CSC-IT Center for Science, Finland, for providing computational resources.

## REFERENCES

- [1] T. Baltrušaitis, C. Ahuja *et al.*, “Multimodal Machine Learning: A Survey and Taxonomy,” *IEEE Transactions on Pattern Analysis and Machine Intelligence*, vol. 41, no. 2, pp. 423–443, 2018.
- [2] K. Ezzameli and H. Mahersia, “Emotion Recognition from Unimodal to Multimodal Analysis: A Review,” *Information Fusion*, p. 101847, 2023.
- [3] M. Muszynski, L. Tian *et al.*, “Recognizing Induced Emotions of Movie Audiences from Multimodal Information,” *IEEE Transactions on Affective Computing*, vol. 12, no. 1, pp. 36–52, 2019.
- [4] Y. Wang, H. Yu, W. Gao, Y. Xia, and C. Nduka, “MGEED: A Multimodal Genuine Emotion and Expression Detection Database,” *IEEE Transactions on Affective Computing*, 2023.
- [5] K. Shingjergji, D. Iren *et al.*, “Interpretable Explainability in Facial Emotion Recognition and Gamification for Data Collection,” in *Int. Conf. on Affective Computing and Intelligent Interaction (ACII)*, 2022, pp. 1–8.
- [6] M. Palash and B. Bhargava, “EMERSK—Explainable Multimodal Emotion Recognition with Situational Knowledge,” *IEEE Transactions on Multimedia*, vol. 1, no. 1, 2023.
- [7] N. Majumder, S. Poria *et al.*, “DialogueRNN: An Attentive RNN for Emotion Detection in Conversations,” in *The 31st AAAI Conference on Artificial Intelligence (AAAI)*, vol. 33, no. 01, 2019, pp. 6818–6825.
- [8] S. Malik, P. Kumar, and B. Raman, “Towards Interpretable Facial Emotion Recognition,” in *The 12th Indian Conference on Computer Vision, Graphics and Image Processing (ICVGIP)*, 2021, pp. 1–9.
- [9] C. Busso *et al.*, “IEMOCAP: Interactive Emotional dyadic MOTion CAPture data,” *Language Resources & Evaluation*, vol. 42, no. 4, 2008.
- [10] L. Tian, M. Muszynski *et al.*, “Recognizing Induced Emotions of Movie Audiences: Are Induced and Perceived Emotions The Same?” in *International Conference on Affective Computing and Intelligent Interaction (ACII)*, 2017, pp. 28–35.
- [11] A. Gaspar and L. A. Alexandre, “A Multimodal Approach to Image Sentiment Analysis,” in *Springer International Conference on Intelligent Data Engineering and Automated Learning (IDEAL)*, 2019, pp. 302–309.
- [12] L. Vadicamo, F. Carrara *et al.*, “Cross-Media Learning for Image Sentiment Analysis in the Wild,” in *IEEE International Conference on Computer Vision Workshops (ICCVW)*, 2017, pp. 308–317.
- [13] E. Jing, Y. Liu *et al.*, “A Deep Interpretable Representation Learning Method for Speech Emotion Recognition,” *Information Processing & Management*, vol. 60, no. 6, p. 103501, 2023.
- [14] J. Lorenzo-Trueba, R. Barra-Chicote *et al.*, “Emotion Transplantation Through Adaptation in HMM-based Speech Synthesis,” *Computer Speech & Language*, vol. 34, no. 1, pp. 292–307, 2015.
- [15] R. Udendhran *et al.*, “Explainable Convolutional Neural Network with Facial Emotion Enabled Music Recommender System,” in *4th Int. Conf. on Information Management and Machine Intelligence (ICIMMI)*, 2022.
- [16] D. Dai, Z. Wu *et al.*, “Learning Discriminative Features from Spectrograms using Center Loss for SER,” in *IEEE International Conference on Acoustics, Speech and Signal Processing (ICASSP)*, 2019, pp. 7405–7409.
- [17] K. Kim and N. Cho, “Focus-Attention-Enhanced Crossmodal Transformer with Metric Learning for MM Speech Emo Recognition,” pp. 1–4, 2023.
- [18] Q. Mao, M. Dong *et al.*, “Learning Salient Features for Speech Emotion Recognition using Convolutional Neural Networks,” *IEEE Transactions on Multimedia*, vol. 16, no. 8, pp. 2203–2213, 2014.
- [19] H. Ma, J. Wang, H. Lin, B. Zhang, Y. Zhang, and B. Xu, “A Transformer-based Model with Self-Distillation for Multimodal Emotion Recognition in Conversations,” *IEEE Transactions on Multimedia*, 2023.
- [20] J. Li, X. Wang *et al.*, “GA2MIF: Graph and Attention based Two-Stage Multi-Source Information Fusion for Conversational Emotion Detection,” *IEEE Transactions on Affective Computing*, 2023.
- [21] A. M. Abubakar *et al.*, “Explainable Emotion Recognition from Tweets using Deep Learning and Word Embedding Models,” in *IEEE 19th India Council International Conference (INDICON)*, 2022, pp. 1–6.
- [22] J. Li, X. Wang *et al.*, “GraphCFC: A Directed Graph based Cross-Modal Feature Complementation Approach for Multimodal Conversational Emotion Recognition,” *IEEE Transactions on Multimedia*, 2023.
- [23] K. Shrivastava, S. Kumar, and D. K. Jain, “An Effective Approach for Emotion Detection in Multimedia Text Data using Sequence based Convolutional Neural Network,” *Multimedia Tools and Applications*, vol. 78, no. 20, pp. 29607–29639, 2019.
- [24] E. Batbaatar, M. Li, and K. H. Ryu, “Semantic Emotion Neural Network for Emotion Recognition from Text,” *IEEE Access*, vol. 7, pp. 111 866–111 878, 2019.
- [25] C. A. Corneanu, M. O. Simón *et al.*, “Survey on RGB, 3D, Thermal, and Multimodal Approaches for Facial Expression Recognition: History, Trends, and Affect-Related Applications,” *IEEE Transactions on Pattern Analysis and Machine Intelligence*, vol. 38, no. 8, pp. 1548–1568, 2016.
- [26] P. Bhattacharya, R. K. Gupta, and Y. Yang, “Exploring the Contextual Factors Affecting Multimodal Emotion Recognition in Videos,” *IEEE Transactions on Affective Computing*, 2021.
- [27] A. R. Asokan, N. Kumar, A. V. Ragam, and S. Shylaja, “Interpretability for Multimodal Emotion Recognition using Concept Activation Vectors,” in *Int. Joint Conf. on Neural Networks (IJCNN)*, IEEE, 2022, pp. 01–08.
- [28] M. R. Makiuchi, K. Uto, and K. Shinoda, “Multimodal Emotion Recognition with High-level Speech and Text Features,” in *IEEE Automatic Speech Recognition and Understanding Workshop (ASRU)*, 2021.
- [29] S. Yoon, S. Byun, and K. Jung, “Multimodal Speech Emotion Recognition using Audio and Text,” in *IEEE Spoken Language Technology Workshop (SLT)*, 2018, pp. 112–118.
- [30] S. Siriwardhana, A. Reis, and R. Weerasekera, “Jointly Fine Tuning ‘BERT-Like’ Self Supervised Models to Improve Multimodal Speech Emotion Recognition,” *INTERSPEECH*, pp. 3755–3759, 2020.
- [31] S. Poria, E. Cambria *et al.*, “Fusing Audio, Visual and Textual Clues for Sentiment Analysis from Multimodal Content,” *Neurocomputing*, vol. 174, pp. 50–59, 2016.
- [32] P. Tzirakis, G. Trigeorgis *et al.*, “End-to-End Multimodal Emotion Recognition Using Deep Neural networks,” *IEEE Journal of Selected Topics in Signal Processing*, vol. 11, no. 8, pp. 1301–1309, 2017.
- [33] T. Zhu, L. Li, J. Yang, S. Zhao, and X. Xiao, “Multimodal Emotion Classification with Multi-Level Semantic Reasoning Network,” *IEEE Transactions on Multimedia*, 2022.
- [34] J. Xie, J. Wang *et al.*, “A Multimodal Fusion Emotion Recognition Method based on Multitask Learning and Attention Mechanism,” *Neurocomputing*, vol. 556, p. 126649, 2023.
- [35] N. Xu, W. Mao, and G. Chen, “A Co-memory Network for Multimodal Sentiment Analysis,” in *ACM International Conference on Research & Development in Information Retrieval (SIGIR)*, 2018.
- [36] M. Shayaninasab and B. Babaali, “Multi-Modal Emotion Recognition by Text, Speech and Video Using Pretrained Transformers,” *arXiv Preprint arXiv:2402.07327*, 2024, Accessed 20 May 2024.
- [37] S. Mai, Y. Zeng, and H. Hu, “Multimodal Information Bottleneck: Learning Minimal Sufficient Unimodal and Multimodal Representations,” *IEEE Transactions on Multimedia*, 2022.
- [38] S. Zhang, Y. Yang *et al.*, “Deep Learning-based Multimodal Emotion Recognition from Audio, Visual, and Text Modalities: A Systematic Review of Recent Advancements and Future Prospects,” *Expert Systems with Applications*, p. 121692, 2023.
- [39] H. Fan *et al.*, “Transformer-Based Multimodal Feature Enhancement Networks for Multimodal Depression Detection Integrating Video, Audio and Remote Photoplethysmograph Signals,” *Information Fusion*, vol. 104, p. 102161, 2024.
- [40] Q. Wei, X. Huang, and Y. Zhang, “FV2ES: A Fully End2End Multimodal System For Fast Yet Effective Video Emotion Recognition Inference,” *IEEE Transactions on Broadcasting*, vol. 69, no. 1, pp. 10–20, 2022.
- [41] G. Hu *et al.*, “UniMSE: Towards Unified Multimodal Sentiment Analysis and Emotion Recognition,” in *PrConference on Empirical Methods in Natural Language Processing*, 2022, pp. 7837–7851.
- [42] R. A. Patamia *et al.*, “Multimodal Speech Emotion Recognition Using Modality-Specific Self-Supervised Frameworks,” in *International Conference on Systems, Man, and Cybernetics*, IEEE, 2023, pp. 4134–4141.
- [43] J. Zhao *et al.*, “MemoBERT: Pre-training Model With Prompt-based Learning for MM Emotion Recognition,” in *International Conference on Acoustics, Speech and Signal Processing (ICASSP)*, 2022, pp. 4703–4707.
- [44] Z. Lian *et al.*, “Mer 2023: Multi-label learning, modality robustness, and semi-supervised learning,” in *Proceedings of the 31st ACM International Conference on Multimedia*, 2023, pp. 9610–9614.
- [45] W. Zheng *et al.*, “Two Birds With One Stone: Knowledge-Embedded Temporal Convolutional Transformer for Depression Detection and Emotion Recognition,” *IEEE Transactions on Affective Computing*, 2023.
- [46] Y. Aytar, C. Vondrick, and A. Torralba, “SoundNet: Learning Sound Representations from Unlabeled Video,” in *Advances in neural information processing systems (NeurIPS)*, 2016, pp. 892–900.



- [47] C. Guanghui and Z. Xiaoping, "Multimodal Emotion Recognition by Fusing Correlation Features of Speech-Visual," *IEEE Signal Processing Letters*, vol. 28, pp. 533–537, 2021.
- [48] P. Kumar, V. Kaushik *et al.*, "Towards the Explainability of Multimodal Speech Emotion Recognition," in *INTERSPEECH*, 2021, pp. 1748–1752.
- [49] S. M. Lundberg and S.-I. Lee, "A Unified Approach to Interpreting Model Predictions," in *The 31st International Conference on Neural Information Processing Systems (NeurIPS)*, 2017, pp. 4768–4777.
- [50] M. B. Fazi, "Beyond Human: Deep Learning, Explainability and Representation," *Theory, Culture & Society*, 2020.
- [51] A. Shrikumar, P. Greenside, and A. Kundaje, "Learning Important Features Through Propagating Activation Differences," in *International Conference on Machine Learning (ICML)*, 2017, pp. 3145–3153.
- [52] L. Shapley, "A Value for n-person Games, Contributions to the Theory of Games II," *Princeton University Press*, 1953.
- [53] J. Castro *et al.*, "Polynomial calculation of The Shapley Value based on Sampling," *Elsevier Computers & Operations Research*, vol. 36, no. 5, pp. 1726–1730, 2009.
- [54] R. Fong, M. Patrick *et al.*, "Understanding Deep Networks Via Extremal Perturbations and Smooth Masks," in *The IEEE/CVF International Conference on Computer Vision (ICCV)*, 2019, pp. 2950–2958.
- [55] M. T. Ribeiro, S. Singh, and C. Guestrin, "Why Should I Trust You? Explaining Predictions of Any Classifier," in *International Conference on Knowledge Discovery & Data Mining (KDD)*, 2016, pp. 1135–1144.
- [56] K. Simonyan *et al.*, "Deep Inside Convolutional Networks: Visualising Image Classification Models and Saliency Maps," in *Proceedings of the International Conference on Learning Representations (ICLR)*, 2014.
- [57] R. R. Selvaraju, M. Cogswell *et al.*, "Grad-CAM: Visual Explanations from Deep Networks via Gradient-based Localization," in *The IEEE/CVF International Conference on Computer Vision (ICCV)*, 2017, pp. 618–626.
- [58] P.-J. Kindermans *et al.*, "The (Un)reliability of Saliency Methods," in *Explainable AI: Interpreting, Explaining and Visualizing Deep Learning*, 2019, pp. 267–280.
- [59] A. Zadeh, P. P. Liang, S. Poria, P. Vij, E. Cambria, and L.-P. Morency, "Multi Attention Recurrent Network for Human Communication Comprehension," in *The AAAI Conference on Artificial Intelligence*, 2018.
- [60] W. Ping, K. Peng *et al.*, "DeepVoice 3: Scaling Text-to-Speech with Convolutional Sequence Learning," in *The 6th International Conference on Learning Representations (ICLR)*, 2018.
- [61] A. v. d. Oord, S. Dieleman *et al.*, "WaveNet: A Generative Model for Raw Audio," *arXiv Preprint arXiv:1609.03499*, 2016, Accessed 20 May 2024.
- [62] Q. You, J. Luo, H. Jin, and J. Yang, "Building a Large Scale Dataset for Image Emotion Recognition: the Fine Print and the Benchmark," in *The AAAI Conference on Artificial Intelligence (AAAI)*, 2016, pp. 308–314.
- [63] K. R. Scherer and H. G. Wallbott, "Evidence For Universality and Cultural Variation of Differential Emotion Response Patterning," *Journal of Personality and Social Psychology*, vol. 66, no. 2, p. 310, 1994.
- [64] R. Plutchik, "The Nature of Emotions: Human Emotions Have Deep Evolutionary Roots, a Fact That May Explain Their Complexity and Provide Tools for Clinical Practice," *Journal Storage Digital Library's American scientist Journal*, vol. 89, no. 4, pp. 344–350, 2001.
- [65] J. Jaiswal, A. Chaubey, and other, "A Generative Adversarial Network Based Ensemble Technique For Automatic Evaluation of Machine Synthesized Speech," in *Asian Conference on Pattern Recognition*. Springer, 2019, pp. 580–593.
- [66] S. Poria, D. Hazarika, N. Majumder, G. Naik, E. Cambria, and R. Mihalcea, "Meld: A Multimodal Multi-Party Dataset For Emotion Recognition in Conversations," *arXiv Preprint arXiv:1810.02508*, 2018, Accessed 20 May 2024.
- [67] K. Simonyan and A. Zisserman, "Very Deep Convolutional Networks for Large-Scale Image Recognition," *arXiv Preprint arXiv:1409.1556*, 2014, Accessed 20 May 2024.
- [68] J. Devlin, M.-W. Chang, K. Lee, and K. Toutanova, "BERT: Pre-training of Deep Bidirectional Transformers for Language Understanding," *arXiv Preprint arXiv:1810.04805*, 2018, Accessed 20 May 2024.
- [69] L. Prechelt, "Early Stopping - But When?" in *Neural Networks: Tricks of the trade*. Springer, 1998, pp. 55–69.
- [70] T.-Y. Lin, P. Goyal *et al.*, "Focal Loss for Dense Object Detection," in *IEEE/CVF Conference on Computer Vision (ICCV)*, 2017, pp. 2980–2988.
- [71] J. Opitz and S. Burst, "Macro F1 and Macro F1," *arXiv Preprint arXiv:1911.03347*, 2019, Accessed 20 May 2024.
- [72] S. M. Vieira, U. Kaymak, and J. M. Sousa, "Cohen's Kappa Coefficient as a Performance Measure for Feature Selection," in *The 18th IEEE International Conference on Fuzzy Systems (IEEE-FUZZ)*, 2010, pp. 1–8.
- [73] D. Ghosal *et al.*, "DialogueGCN: A Graph Convolutional Neural Network for Emotion Recognition in Conversation," in *Conference on Empirical Methods in Natural Language Processing*, 2019, pp. 154–164.
- [74] D. Hu, L. Wei, and X. Huai, "DialogueCRN: Contextual Reasoning Networks for Emotion Recognition in Conversations," in *Annual Meeting of the Association for Computational Linguistics*, 2021, pp. 7042–7052.
- [75] D. Hu *et al.*, "MM-DFN: Multimodal Dynamic Fusion Network For Emotion Recognition In Conversations," in *Int. Conference on Acoustics, Speech and Signal Processing (ICASSP)*. IEEE, 2022, pp. 7037–7041.
- [76] P. Kumar, V. Khokher, Y. Gupta, and B. Raman, "Hybrid Fusion based Approach for Multimodal Emotion Recognition with Insufficient Labeled Data," in *The 28th IEEE International Conference on Image Processing (ICIP)*, 2021, pp. 314–318.
- [77] V. Lopes, A. Gaspar, L. A. Alexandre, and J. Cordeiro, "An AutoML-based Approach to Multimodal Image Sentiment Analysis," in *The International Joint Conference on Neural Networks (IJCNN)*. IEEE, 2021, pp. 1–9.
- [78] R. Deng, C. Shen, S. Liu, H. Wang, and X. Liu, "Learning to Predict Crisp Boundaries," in *The European Conference on Computer Vision (ECCV)*, 2018, pp. 562–578.



and conferences and received various awards, including the institute medal in M.E., the best thesis award, and several best paper awards. For more information, visit his webpage at [www.puneetkumar.com](http://www.puneetkumar.com).



For more details, visit his webpage at [www.linkedin.com/in/sarthak-malik](http://www.linkedin.com/in/sarthak-malik).



For more information, visit his webpage at <http://faculty.iitr.ac.in/cs/bala>.



For more information, visit her webpage at [www oulu.fi/en/researchers/xiaobai-li](http://www oulu.fi/en/researchers/xiaobai-li).

**Puneet Kumar** (Member, IEEE) received his B.E. and M.E. degrees in Computer Science in 2014 and 2018, respectively, and his Ph.D. from the Indian Institute of Technology Roorkee, India in 2022. He has worked at Oracle Corporation, Samsung R&D, and PaiByTwo Pvt. Ltd., and is now a Postdoctoral Researcher at the University of Oulu, Finland. His research interests include Affective Computing, Multimodal and Interpretable AI, Mental Health, and Computational Cognitive Neuroscience. He has published in top journals

**Sarthak Malik** received his B.Tech degree in Electrical Engineering from the Indian Institute of Technology Roorkee, India. He is currently a Data Scientist at MasterCard. He is an avid programmer and an active participant in coding competitions and development projects. His research focuses on Affective Computing, Computer Vision, and Interpretable AI. He has published in reputed journals and conferences and achieved notable recognitions, including a rank in the top 10 in the Geoffrey Hinton Fellowship hackathon.

**Balasubramanian Raman** (Senior Member, IEEE) received his B.Sc. and M.Sc. degrees from the University of Madras in 1994 and 1996, respectively, and his Ph.D. from the Indian Institute of Technology Madras, India in 2001. He is a Chair Professor in the Department of Computer Science and Engineering and a Joint Faculty in the Mehta Family School of Data Science and Artificial Intelligence at the Indian Institute of Technology Roorkee, India. He has published over 200 research papers in reputed journals and conferences. His research interests include Machine Learning, Image and Video Processing, Medical Imaging, Computer Vision, and Pattern Recognition.

**Xiaobai Li** (Senior Member, IEEE) received her B.Sc. and M.Sc. degrees in 2004 and 2007, respectively, and her Ph.D. from the University of Oulu, Finland, in 2017. She is currently a ZJU100 professor with the School of Cyber Science and Technology, Zhejiang University, and she is also an Adjunct Professor with the Center for Machine Vision and Signal Analysis, University of Oulu. Her research focuses on Affective Computing, Facial Expression Recognition, Micro-Expression Analysis, Remote Physiological Signal Measurement, and Healthcare. She co-chaired several international workshops in CVPR, ICCV, FG, and ACM Multimedia and is an Associate Editor of IEEE Transactions on Circuits and Systems for Video Technology, Frontiers in Psychology, and Image and Vision Computing.